Molecular Dynamics of "Hairy Rod" Molecules in the Solid State: Poly(γ-methyl L-glutamate)-*co*-(γ-*n*-octadecyl L-glutamate) in Solution-Cast Films

A. Schmidt,* S. Lehmann, M. Georgelin,† G. Katana,‡ K. Mathauer,§ F. Kremer,|| K. Schmidt-Rohr, C. Boeffel, G. Wegner, and W. Knoll⊥

Max-Planck-Institut fuer Polymerforschung, P.O. Box 3148, D-55021 Mainz, Germany

Received January 17, 1995; Revised Manuscript Received April 5, 1995⊗

ABSTRACT: We present the thermal, structural, and dynamic properties of poly(γ-methyl L-glutamate)-*co*-(γ-octadecyl L-glutamate) with 30% octadecyl chains in solution-cast films. This substance is an example of a so-called "hairy rod" molecule. The peptide backbones form stiff rods which are surrounded by the side chains. The structure of the solution-cast film was measured by WAXS and SAXS. We found amorphous and crystalline side chain parts. The melting point of the crystalline side chains is ca. 293 K. The thermal properties of these "hairy rods" are investigated with differential scanning calorimetry, and the dynamic properties are measured between 110 and 370 K with broad-band dielectric spectroscopy (10^{-2}−10^{9} Hz) and variable-temperature ^{13}C-CP/MAS solid-state NMR. Three dielectric-active relaxation processes are observed: Two processes have a temperature dependence according to the Williams−Landel−Ferry (WLF) equation. They approach each other with decreasing temperature and merge at about 238 K, i.e., the calorimetric glass transition temperature. These two processes are discussed as fluctuations of the main chain and the surrounding side chain groups. The third relaxation process has an Arrhenius-type temperature dependence with an activation energy of 43 kJ/mol. It is assigned to fluctuations of the carboxyl groups in the side chains. The variable-temperature NMR results confirm that one of the WLF-type relaxations is caused by the side chains. These NMR experiments also show that the main chains undergo no local relaxation in the investigated temperature and frequency region and stay in the α-helix conformation.

1. Introduction

Rodlike polymers with covalently attached flexible side chains, so-called "hairy rod" molecules, have been developed during the past decade. This type of molecule is of interest because it can be spread on a LB trough and compressed to a 2D-nematic liquid crystal. The resulting monolayer can be transferred to solid substrates, and multilayers can be formed. The resulting structure consists of stiff rods embedded in a matrix of flexible side chains. Different chemical designs of "hairy rod" polymers and applications of the resulting supramolecular architectures can be found in the recent review by Wegner.[1] "Hairy rods" are also of interest because of their liquid-crystalline behavior in bulk. The flexible side chains act as a solvent skin to the molecules and give them thermotropic properties.[2]

Copolyglutamates with alkyl side chains are one example of such "hairy rod" molecules. In particular, poly(γ-methyl L-glutamate)-*co*-(γ-octadecyl L-glutamate) with 30% long side chains[3] (see Figure 1a; we use OM-30 for abbreviation) is often used for LB applications.[1] We previously measured the dynamics of the rods by determining the diffusion between the monolayers in the Langmuir−Blodgett films of OM-30.[4] The goal of this paper is to investigate the molecular dynamics in the main and side chains of the molecules in thin films prepared by solution casting. The results obtained with these thin films (30−50 μm) of OM-30 represent the bulk properties of the material. The understanding of the dynamics in the bulk polyglutamate will help us to understand the properties of LB films and devices made from these supramolecular architectures.

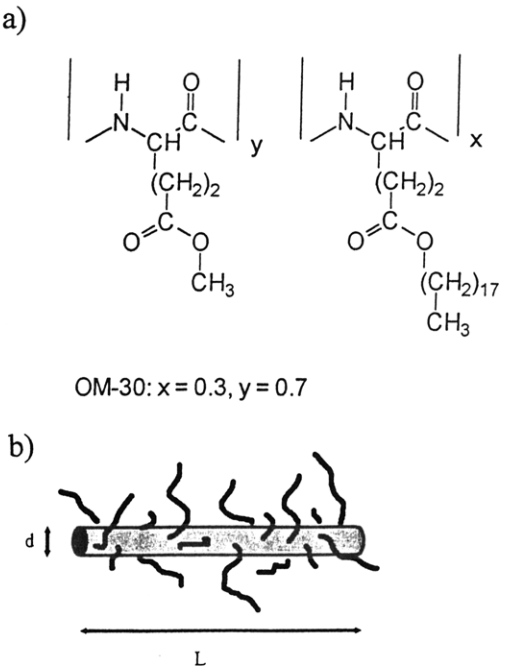

Figure 1. (a) Chemical structure of the molecule OM-30. (b) The peptide main chain in OM-30 forms an α-helix that acts as a rod of length L and diameter d. The attached long and short side chains around the main chain like a solvent skin.

† Present address: Laboratoire de Recherche en Combustion, Universite de Provence, Avenue Escadrille Normandie-Niemen, 13397 Marseille Cedex 13, France.

‡ Present address: Department of Physics, Kenyatta University, P.O. Box 43844, Nairobi, Kenya.

§ Present address: BASF AG, Kunststofflaboratorium, D-6700 Ludwigshafen, Germany.

|| Present address: Fakultaet fuer Physik und Geowissenschaften, Universitaet Leipzig, Linnestrasse 5, D-04103 Leipzig, Germany.

⊥ Also with The Institute of Physical and Chemical Research, Frontier Research Program, 2-1 Hirosawa, Wako-Shi, Saitama 351-01, Japan.

⊗ Abstract published in *Advance ACS Abstracts,* May 15, 1995.

0024-9297/95/2228-5487$09.00/0

We will first summarize what is already known about the structure and dynamics of homo- and copolyglutamates. There are two general types of structures and dynamics reported for polyglutamates with alkyl side chains in the solid state. In the first one (type I) the rods build up a layered structure, with the side chains stretched away from these layers in both directions and forming an alkyl chain crystal.[2b] Beyond the melting point of this side chain crystal the rods show a complex thermotropic liquid-crystalline behavior.[2b] In the second type (type II) the rods form a hexagonal structure, while the side chains surround each helix backbone symmetrically.[5] The side chains are in a glassy state in this structure.[6] The rods undergo rotational and translational motions at elevated temperatures.[2b,9] Homopolyglutamates with alkyl side chains form the type II structure if the chain length is smaller than 10 carbon atoms, while for longer alkyl chains the homopolymers form the first type with the crystallizing side chains.[2b] Poly(γ-benzyl L-glutamate) (PBLG) also forms a type II structure.[7] Copolymerization of glutamates with alkyl chains of different length, or of alkyl chains and benzyl glutamates, do not change the above finding if both side chains are shorter than 7 carbon atoms.[2a,6] There are detailed investigations about the dynamics in homopolymers of type I[2b,8] and II,[6,9,8d] especially in PBLG.[7b,10] The dynamics in copolymers of type II with two short side chains is also known.[2a,6,11]

This paper deals with the polymer OM-30, where the related homopolymers poly(methyl L-glutamate) (PMLG) and poly(octadecyl L-glutamate) (POLG) form opposite types of structures. To our knowledge the dynamics in this copolyglutamate OM-30 has not been investigated in detail. A series of molecules OM-x, where x stands for the percentage of long octadecyl chains, were investigated with differential scanning calorimetry (DSC) and wide-angle X-ray scattering (WAXS) by Tsujita et al.[12] From these investigations with polymers for OM-82 to OM-52 they determined that only copolyglutamates with x greater than 35% form side chain crystals. Their WAXS data are in agreement with a type I structure for OM-x, with x from 52 to 82.[12b] These investigations predict that the side chains in OM-30 are not in a crystalline state.[12b]

In a study by Yamaguchi et al. the structure and molecular motion of the side chains were investigated for OM-83, -62, -38, and -25 by DSC, NMR, and a spin-probe technique.[13] In this report it was found that all the measured OM-x's have long side chains which are partly crystalline below the melting point, but a fraction of the side chains are amorphous below the melting point. Above the melting point the long side chains are liquidlike and highly mobile. We will compare the model developed in ref 13 with our measurements of the dynamics in OM-30.

Our investigation focuses on the quantitative determination of the molecular dynamics of both the main chain and the side chains, especially the region close to the α-helix. We first investigated the structural and thermal properties of OM-30 by DSC, WAXS, and small-angle X-ray scattering (SAXS). The molecular dynamics was measured with broad-band dielectric spectroscopy (DS) and solid-state nuclear magnetic resonance (NMR) in the range between 110 and 370 K. DS offers the possibility of measuring relaxation parameters of dipoles over a broad time scale. Solid-state NMR allows the investigation of the conformation and dynamics of specific carbon atoms. Therefore solid-state NMR is complementary to WAXS and DS for our purposes.

2. Experimental Section

Material. Poly(γ-methyl L-glutamate)-*co*-(γ-octadecyl L-glutamate) with 30% long side chains (OM-30) is used for this investigation (Figure 1a). The synthesis of OM-30 with an average molecular weight of 460 000 (determined by light scattering) and a degree of polymerization of 2100 (OM-30-2100) is described in ref 14. For the dielectric spectroscopy we also used OM-30 with a smaller molecular weight of 210 000 and a degree of polymerization of 960 (OM-30-960).[3] The molecular weight distribution for both polymers is unknown. We use OM-30 for the polymer OM-30-2100 through the remainder of this text and refer to OM-30-960 and OM-30-2100 when necessary.

The peptide backbones of the polyglutamates form an α-helix with a diameter, d, of 0.56 nm (not including $(CH_2)_2$ and the ester groups), 3.6 residues per pitch, and a pitch height of 0.54 nm (see Figure 1b).[15] The average contour length, L, of OM-30 is therefore 320 nm (150 nm for the lower molecular weight). The average molecular weight and radius of gyration (64 nm) were determined by light scattering experiments for OM-30.[16] The persistence length of the molecule could be approximated from this experiment to be 110 nm.[17] The α-helix acts therefore not really as a stiff rod, but is a Kratky–Porod worm[18] for both polymers. The alkyl chains are attached covalently to the main chain. The length, l, of the all-trans octadecyl chain would be 2.3 nm.[3]

Sample Preparation. A 2% w/w solution of OM-30 in chloroform (UVASOL, Merck) was prepared and cast on gold-plated brass or Teflon plates. These plates were kept in a closed jar in a saturated chloroform atmosphere for 5 days. The jar was then opened, and the OM-30 film was allowed to dry for 1 day and then annealed in a vacuum oven at 353 K for 12 h. The film thicknesses after drying are about 30–50 μm, measured with a mechanical tip. For the dielectric spectroscopy samples a thin gold layer of 100 nm thickness was evaporated on top of the film as an electric contact. The films for the WAXS and NMR investigations were stripped from the Teflon surface.

The **differential scanning calorimetry** (DSC) measurements were carried out with a Mettler DSC-30. The mass of the sample was 13.1 mg and the heating rate was 5 K/min.

The **wide-angle X-ray scattering** (WAXS) experiments were performed with a rotating anode (Rigaku RV-300, 18 kW), using the Cu Kα line ($\Delta\lambda/\lambda = 0.014$). The beam divergence was set by two slits at 0.056°. The diffraction pattern was measured with a Nicolet two-dimensional detector of 512 × 512 pixels. The distance between the sample and detector was 110 mm, allowing a resolution of 0.14 nm^{-1} and a maximal momentum transfer of 34 nm^{-1}.

A Kratky camera[19] (Anton-Paar) was used for the **small-angle X-ray scattering** (SAXS). Here also the Cu Kα line was chosen for the experiments. The beam divergence was set to be 0.095°. A one-dimensional position-sensitive detector (Braun) allowed the resolution of 0.02° in the diffraction pattern and enabled the investigation of momentum transfers from 0.6 to 3.5 nm^{-1}. The raw data were collected for absorption, smearing, and background.[20]

The **dielectric spectroscopy** (DS) experiments in the frequency range between 10^{-2} and 10^9 Hz were carried out by measuring the complex impedance of a sample-filled capacitor. The capacitor consisted of two gold-plated brass disks. The lower one, on which the polyglutamate film was prepared by solution casting, had a diameter of 20 mm, while the upper one had a diameter of 5 mm and was pressed on the thin sample film.

A Solartron Schlumberger frequency response analyzer FRA 1254 covered the frequency range from 10^{-4} to 6×10^4 Hz.[21,22] In the audio frequency range ($10-10^7$ Hz) a Hewlett-Packard 4192A impedance analyzer was used. For the range between 10^6 and 10^9 Hz the Hewlett-Packard 4191A analyzer was employed, which is based on the reflectometer principle. Here the lower and upper brass plates were only 5 mm in diameter.

The relative accuracy of the measurements for samples with a dielectric loss of 10^{-2} is 1% in ϵ' and 3% in ϵ''. The temperature during measurements was controlled by a custom-made cryostat, which allows adjustment of the sample temperature from 110 to 410 K. This was achieved by using a temperature-controlled nitrogen gas flow, with an accuracy of 0.05 K.[22]

With DS relaxation processes of dipoles and space charging can be investigated. In the case of OM-30 there are two groups which contribute significantly to dipole relaxation. The first one is located within the helix backbone and consists of the amide group HNCO. The second one is the ester group in the side chain. Investigations of different polyglutamates showed that the net dipole moment of these polypeptides is nearly parallel to the rod, having an angle of only 2° with the rod direction.[23] The dipole moment of the single HNCO dipole is about 3.7 D, and the dipole moment of an ester group is about 1.8 D.[24]

The dispersion of the complex dielectric function $\epsilon^* = \epsilon' + i\epsilon''$ can be described by the Havriliak–Negami equation[25]

$$\epsilon' = \epsilon_\infty + \frac{\epsilon_{st} - \epsilon_\infty}{(1 + (i\omega\tau)^p)^q} \tag{1}$$

in the frequency domain. ϵ_{st} stands for the static dielectric function at $\omega\tau \ll 1$ and ϵ_∞ is the real part of ϵ^* at high frequencies ($\omega\tau \gg 1$). The parameter τ is the mean relaxation time of the dielectric process. The parameters p and q, with $0 < p,q \leq 1$, describe the symmetric and asymmetric broadening of the relaxation time distribution. The parameter p characterizes the logarithmic slope at low frequencies and the product pq the slope on the high-frequency side. Broad relaxation time distributions are therefore described by small values of p and q. The resulting spectra measured at different temperatures were fitted with the Havriliak–Negami function, and the parameters p, q, and τ and the relaxation strength $\Delta\epsilon$, defined as $\Delta\epsilon = \epsilon_{st} - \epsilon_\infty$, were obtained. The errors for $\Delta\epsilon$ and τ are about 10%.

The relaxation strength $\Delta\epsilon$ depends on the total electric dipole moment μ of the monomer unit and the number density N of dipoles:[26]

$$\Delta\epsilon = \frac{\delta N\langle\mu^2\rangle}{9k_{B_T}\epsilon_0}\frac{\epsilon_{st}(\epsilon_\infty + 2)^2}{2\epsilon_{st} + \epsilon_\infty} \tag{2}$$

Here the Kirkwood–Froehlich correlation parameter δ describes the correlation between different dipoles. For non-correlated systems ($\delta = 1$) eq 2, known as the Froehlich equation, is reduced to the Onsager equation.[27]

At frequencies below 10^3 Hz a conductivity contribution adds to the measured dielectric loss.[28] It obeys the power law

$$\epsilon'' = \frac{\sigma_0}{\epsilon_0}\omega^{s-1} \tag{3}$$

where σ_0 and s are fit parameters. Since the relaxation process and the conductivity contribution strongly differ in their functional form, the two can be easily separated. If two processes occurred in the frequency window of the experiment a twofold Havriliak–Negami function plus a conductivity contribution were fitted to the experimental data.

There are typically two possibilities for the temperature dependence of the mean relaxation time τ in polymers. The relaxation time can show an Arrhenius behavior

$$\tau = \tau_0 \exp(E/RT) \tag{4}$$

or can follow a Vogel–Fulcher equation

$$\tau = \tau_0 \exp\left(\frac{A}{T - T_V}\right) \tag{5}$$

Here E is an activation energy, R is the gas constant, A is a constant, T_V is the Vogel–Fulcher temperature, and τ_0 is a characteristic time constant. Equation 5 describes phenomena related to a glass transition. It is more convenient for data evaluation to write the Vogel–Fulcher equation in the form of the Williams–Landel–Ferry (WLF) equation,[29] where the relaxation times at different temperatures are compared.

$$\log\left(\frac{\tau_1}{\tau_2}\right) = \frac{C_1(T_2 - T_1)}{C_2 + (T_2 - T_1)} \tag{6}$$

The parameters C are related to the activation energy and the Vogel–Fulcher temperature by $C_2 = (T_1 - T_V)$ and $C_1 = (\log e)A/C_2$. The experimental values T_1 and τ_1 are kept constant for the fit and T_2 and τ_2 are varied.

Solid-State NMR. For the study of conformation and dynamics of poly(amino acids) solid-state NMR was employed. Many authors have reported on various NMR experiments in the solid state, such as variable-temperature (VT) ^{13}C-CP/MAS-NMR,[8a,11,30] ^{1}H-NMR relaxation time measurements,[8b] and ^{2}H-NMR studies.[31] In this work VT-^{13}C-CP/MAS experiments were performed in order to study changes in dynamics and conformational order of both the side chains and the α-helical backbone.

All solid-state NMR experiments were performed on a Bruker MSL 300 spectrometer at a ^{1}H resonance frequency of 300.13 MHz and a ^{13}C frequency of 75.47 MHz. The temperature was changed in steps of 5 or 10 K and controlled by a home-built VT unit. The experiments were carried out using a double-bearing VT Bruker MAS probe head and 7 mm zirconium oxide rotors. The parameters for the different experiments were as follows: The sample-containing rotor was spun at 4 kHz, or at 1 kHz for the low spinning frequency experiment, using a cross polarization time of 3 ms and a recycle delay of 5 s. Dwell time and total number of data points were 22 μs and 2000, respectively. The number of accumulations was 512 scans. The chemical shifts were calibrated using external adamantane (38.5 ppm relative to TMS).

3. Results

The result of a **WAXS** experiment at 260 K is shown in Figure 2. The beam impinged perpendicular to the film surface. It is known that the rods will lay parallel to the substrate surface,[7a] therefore the nearly isotropic 2D-intensity distribution (Figure 2a) indicates that the rods are not all aligned in one direction, but different domains are formed, with a nearly rotation symmetric distribution of the domain directors. Two Bragg peaks are visible at $(2\pi/2.86)$ and $(2\pi/1.05)$ nm^{-1} in the angle integrated intensity in Figure 2b. It is possible to fit the two peaks as (100) and (210) for a hexagonal structure, with a nearest-neighbor distance between rods of 3.3 nm, but two Bragg peaks are not significant to determine a structure. All that can be concluded from this measurement is a spacing of 2.86 nm between two layers of helices. Similar distances were found in the hexagonal phase of type I homo- and copolyglutamates.[2b,12b] The full width at half-maximum (fwhm) of the first Bragg peak indicates a correlation length of 5.6 nm.

The side chains are visible beyond 8 nm^{-1}. The broak peak at 14.3 nm^{-1} agrees with the 0.44 nm distance of a triclinic alkane lattice.[2b] This peak is superimposed onto a broad halo from 8 to 19 nm^{-1}. The presence of this peak proves that the side chains are not completely disordered at this temperature. The ratio between the areas under the peak and the halo is ca. 0.25. The Scherrer equation allows one to calculate from the fwhm a correlation length of 2.8 nm, which means that only about 6 chains are correlated.

The first Bragg peak at 2.20 nm^{-1} was investigated further with a **SAXS** experiment as a function of

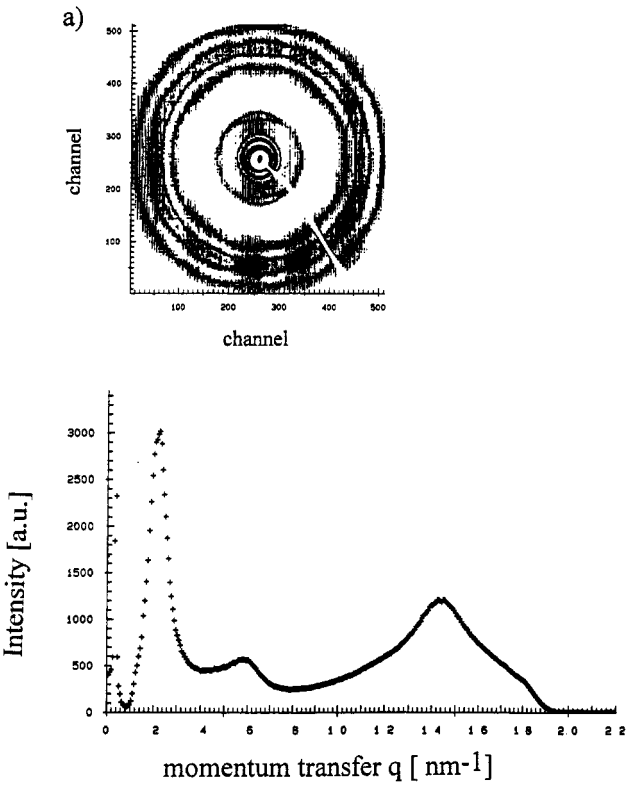

Figure 2. (a) Isointensity lines of a 2D-WAXS experiment with OM-30-2100 at 260 K. (b) The radial integrated intensity consists of two Bragg peaks for the rods and a Bragg peak superimposed onto a broad halo for the alkyl chains (8–19 nm^{-1}).

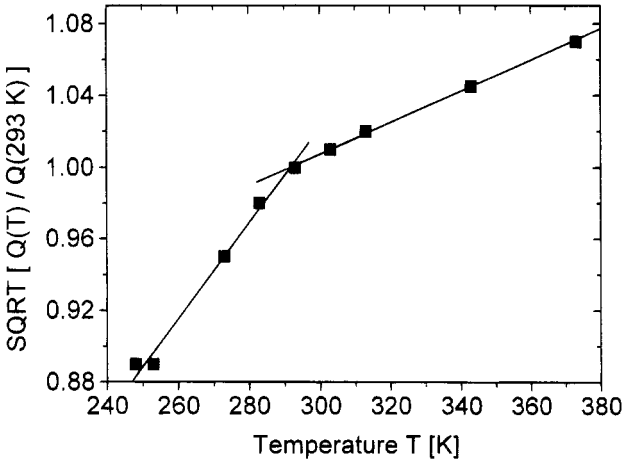

Figure 3. Normalized square root of the integral invariant Q of the Bragg peak at 2.20 nm^{-1} as a function of temperature as measured by SAXS. The two full lines show the linear fit of the data. The error is approximately the size of the symbol.

temperature from 248 to 373 K. The peak position and the full width at half-maximum did not change within the experimental errors, but the peak area grows with increasing temperature. The peak area Q, which is proportional to the integrated square of the electron density,[32] was evaluated. The normalized square root of this invariant Q is shown in Figure 3. The points can be connected by two straight lines, which change slope at 293 K. The ratio of the slope before and beyond 293 K is 2.8/1.0.

The **DSC** curve (see Figure 4) of OM-30 shows a transition at 140 K (γ-process) and a very broad process (called β) with no distinct peak. The β-transition starts between 230 and 240 K and its minimum is at 273 K.

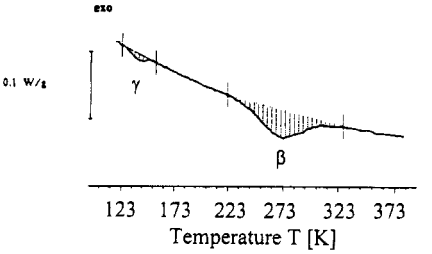

Figure 4. DSC curve of OM-30-2100. The mass of the sample was 13.10 mg and the heating rate was 5 K/min. Two transitions around 140 K (γ-process) and from 220 to 320 K (β-process) are visible.

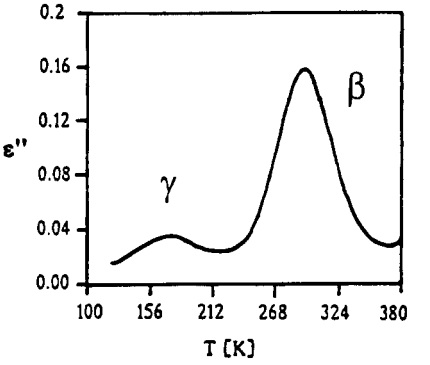

Figure 5. Dielectric loss ϵ'' of OM-30-2100 at 100 kHz as a function of the sample temperature between 120 and 380 K. Two processes β and γ are present.

The shape of this curve is similar to the reported data for OM-38 and OM-25.[13] Beyond the melting point of the crystalline side chains in POLG and also in copolymers with different alkyl chains, Watanabe et al. found thermotropic behavior.[2] The bulk samples of OM-30 do not show liquid-crystalline phases in DSC and in polarized light microscopy between 290 and 370 K.[16]

To learn about the dynamic properties **broad-band dielectric spectroscopy** from 10 mHz to 1 GHz in the temperature region from 110 to 380 K was done. Figure 5 shows as an example of the experimental results the dielectric loss ϵ'' at 100 kHz as a function of temperature. There are two processes observable, similar to the DSC curve in Figure 4: a small γ-process with a maximum at 170 K and a stronger β-process with a maximum at 295 K. Similar processes were found in PMLG and PBLG and different copolyglutamates, measured by DS,[6,7b,8c,10a–c] viscoelastic experiments,[2a,b] and NMR.[8a,b,d,10d,13]

For all measured frequencies and temperatures the permittivity ϵ' is between 3 and 4 for OM-30-2100 and between 12 and 16 for the smaller molecule OM-30-960. The maximum dielectric loss ϵ'' is equal to 0.16 for OM-30-2100, while the low molecular weight polymer has a maximum loss of 0.5.

The maxima of the loss peaks are shifted with increasing temperature to higher frequencies. By changing the temperature, each process can so be shifted into the frequency window of the dielectric spectrometer. Below 160 K only the γ-relaxation is in the frequency window. The fit of the experimental data was possible with one Havriliak–Negami function and a conduction term. The width parameters from this fit are $p = 0.25$ and $q = 0.75$ with a typical error of 15%.

With increasing temperature the γ-process is moving out of the frequency window of our experiment and the β-relaxation is moving in. At 230 K only the β process is present. Increasing the temperature over 260 K a

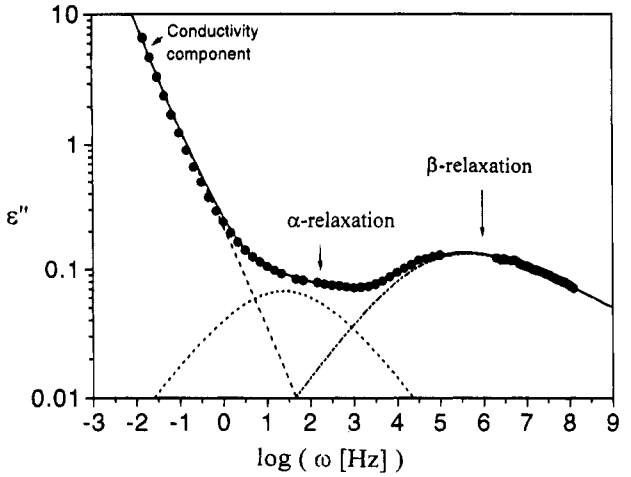

Figure 6. Dielectric loss ϵ'' of OM-30-2100 at 293 K as a function of the frequency. The experimental data (full dots) can be fitted (full line) by a conductivity contribution and two relaxations (broken lines), called α and β. The size of the symbol is approximately the experimental error.

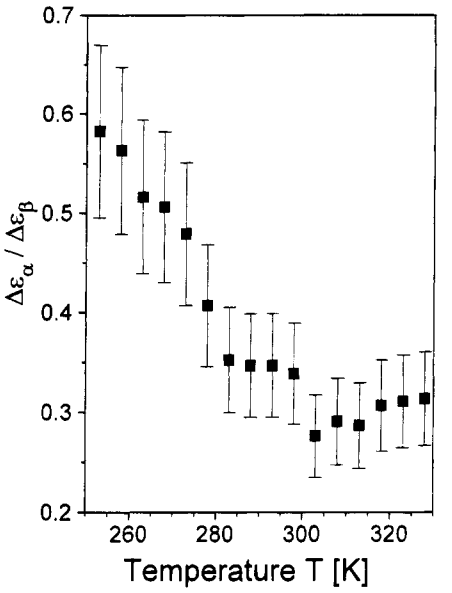

Figure 7. Ratio $\Delta\epsilon_\alpha/\Delta\epsilon_\beta$ of the two relaxation strengths of the α- and β-processes as a function of the temperature between 250 and 330 K. The ratio decreases between 250 and 280 K and is constant within the experimental error beyond 285 K with a value of 0.32 ± 0.08.

third process, α, appears. Figure 6 shows an example of the evaluation of the data at 293 K, where both α- and β-processes are visible. The experimental curve can be fitted by one conductivity term and two relaxation processes. The dashed lines are the three different contributions of the fit, while the solid line is the sum of all three functions compared to the experimental data (black dots). The width parameters p and q are 0.25 and 0.75, respectively, with a typical error of 15%. The β-process is faster by a factor of 1000 compared to the α-relaxation over the whole temperature range and has a higher loss and bigger relaxation strength $\Delta\epsilon$. The relaxation strength $\Delta\epsilon_\beta$ of the β-process increases with increasing temperature and stays constant after the temperature has reached 285 K. The relaxation strength $\Delta\epsilon_\alpha$ of the α-process is also constant (and larger than zero) beyond 285 K, and the ratio $\Delta\epsilon_\alpha/\Delta\epsilon_\beta$ is equal to 0.32 ± 0.08. Figure 7 shows the ratio $\Delta\epsilon_\alpha/\Delta\epsilon_\beta$ as a function of the temperature.

Figure 8 summarizes the dielectric results. The

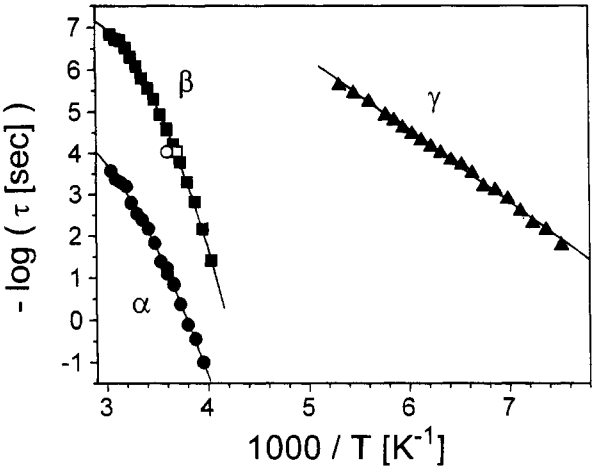

Figure 8. Arrhenius plot of the mean relaxation time τ of the processes α, β, and γ in the polymer OM-30-2100 as determined from dielectric spectroscopy. The solid lines are the fits to the data points. The open square is the result for the side chain dipole found by NMR. The frequency of the OCH_3 and OCH_2 groups, also measured by NMR, is shown as an open circle. The size of the symbols represents approximately the experimental error.

Table 1. Fit Parameters[a] for the Dielectric Relaxations (Eqs 4 and 5)

process	E (kJ/mol)	τ_0 (s)
γ	43 ± 1	$10^{-(16.7\pm0.1)}$

process	A (K)	τ_0 (s)	T_V (K)	T_g (K) $\omega(T_g) = 10$ mHz
β	529 ± 24	$10^{-(11.2\pm0.2)}$	194 ± 3	236 ± 4
α	2285 ± 481	$10^{-(9.5\pm0.6)}$	157 ± 10	240 ± 17

[a] All values are a weighted average over different samples.

evaluated relaxation times τ are plotted as a function of the inverse temperature. The γ-process can be fitted with a straight line in this kind of plot. Therefore this process follows Arrhenius behavior. The linear fit gives an activation energy E of 43 kJ/mol and a preexponential factor τ_0 of $10^{-16.7}$ s. This γ-process was also measured in polyglutamates with different side chains,[6,8b,d,10a] and from NMR[8b] and viscoelastic measurements[2b] activation energies of 42–46 kJ/mol are reported. This relaxation is explained as a restricted twisting motion of the carboxyl dipoles in the side chains.[2b]

The α- and β-processes cannot be fitted by a straight line in an activation plot. The temperature dependence of these relaxations can be described with a Vogel–Fulcher equation or a WLF fit. The fit parameters are given in Table 1 and result from weighted averages over the results from different samples. Both relaxations describe dynamic glass transitions. The two WLF processes approach each other with decreasing temperature and merge at about 238 K. The calorimetric glass transition temperature T_g is related to the dynamical glass transition and can be approximated as the temperature at which the relaxation frequency is equal to 10 mHz. The so-approximated calorimetric glass temperatures T_g are also given in Table 1. Within the limits of experimental accuracy T_g is identical for both relaxations and equal 238 K. This value agrees with the onset in the second transition in the DSC measurements. The β-relaxation is faster than the α-process and the parameter A for the α-process is larger by a factor of 5, while the Vogel–Fulcher temperature is smaller.

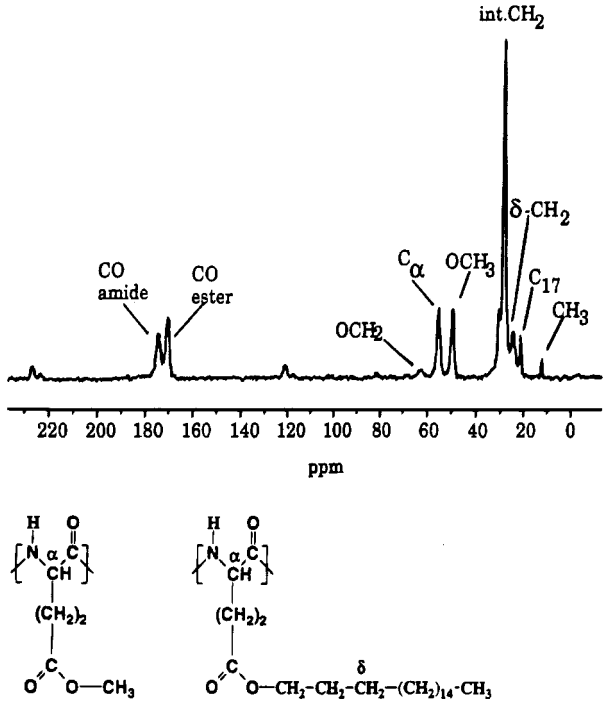

Figure 9. ^{13}C-CP/MAS-NMR of OM-3-2100 measured at 295 K. The inset shows the chemical structure of the molecule and the peak assignment to the respective sites in the molecule. Adamantane is used as external reference, and the sample was spun at 4 kHz.

The Greek letter β is typically used for Arrhenius type relaxations in the dielectric literature. The polyglutamate literature names the relaxation with Greek letters in alphabetic order as the temperature of the process decreases. We follow the latter practice in this paper.

We also investigated the relaxations of the lower molecules weight polymer OM-30-960. The results for the activation energies, transition temperatures, and relaxation frequencies are, within experimental errors, identical to the results for OM-30-2100. The only difference is that the relaxation strength of all three processes is larger by a factor of ca. 10 for the polymer with the lower molecular weight.

To confirm the assignment of relaxation processes from the dielectric spectroscopy experiments, **^{13}C solid-state NMR** was employed, where it is possible to distinguish between different sites of the molecules because of the chemical shift resolution of the ^{13}C spectra. VT-^{13}C-CP/MAS-NMR also allows investigation of the structure and dynamics of other parts of the molecule.

In Figure 9 the ^{13}C-CP/MAS-NMR measured at 295 K is shown with all peaks identified (inset). Starting at 0 ppm, one first can identify the carbon atom of the long alkyl side chain, with the methyl group (C_{18}) at the highest field. The largest peak (~30 ppm) belongs to the interior CH_2 groups of the long alkyl chains. The chemical shift of the interior CH_2 groups is dependent on the conformational environment of these groups, i.e., whether the chain adopts an all-trans or mostly gauche conformation. Due to the γ-gauche effect the chemical shift of the methylene groups in an all-trans conformation is about 3–4 ppm higher than in a situation of mostly gauche conformations.[33] The peaks at ~52 and ~65 ppm belong to OCH_3 and OCH_2, respectively, whereas the peak at ~57 ppm is assigned to the C_α carbon in the main chain. Of special interest in order

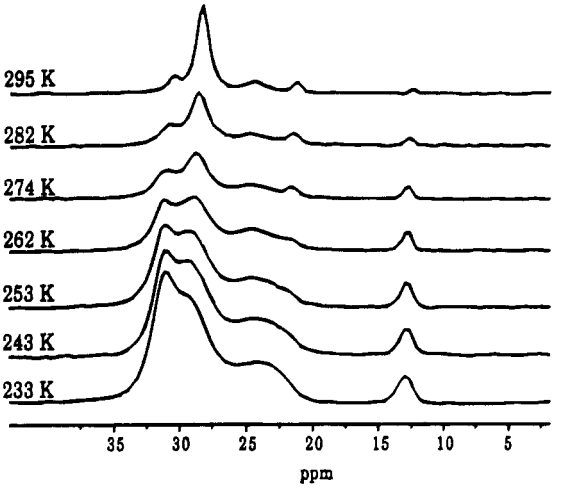

Figure 10. VT-^{13}C-CP/MAS-NMR of the alkyl part of OM-30-2100 between 233 and 295 K. Adamantane is chosen as external reference. This experiment shows the melting of the octadecyl side chains.

to answer the question of which dipole is responsible for the relaxation behavior are the two carbonyl peaks at 172.5 (side chain ester) and 175.8 ppm (main chain amide). The chemical shifts of the C_α and CO amide peaks are characteristic for an α-helix.[11] The position of the ester peak is nearly identical with that in PBLG,[11] meaning the ester group is in a similar conformation in both PBLG and OM-30.

Figure 10 shows the alkyl part of the NMR spectra measured as a function of temperature from 233 to 295 K. All changes in position or shape of the peaks are smooth. The temperature dependence of the chemical shifts can be found in Table 2. The most significant change can be observed at the position of the interior side chain CH_2 groups. The continuous decrease of the lower field portion of the peak at ~32.5 ppm (all-trans conformation) and the simultaneous increase of the higher field portion at ~30.5 ppm (gauche conformation) hint at some melting process of the side chains. In comparison to measurements on a similar system[8a] (POLG, which contained purely octadecyl side chains) the chemical shifts for the all-trans peak in OM-30 is smaller. This shows that in OM-30 the side chains are not in a highly crystalline surrounding. Nevertheless, the difference of more than 2 ppm between the "all-trans" peak and the gauche peak is significant.[33] The ratio of all-trans to gauche conformations becomes smaller with increasing temperature with the largest all-trans portion at the lowest temperature. Also, the chemical shift of the gauche portion of the peak changes by ~0.7 ppm over the measured temperature range. The reason for that is the increasing amount of gauche population. It is only possible to give a qualitative estimation of the all-trans to gauche ratios out of CP/MAS spectra due to the dependence of the cross-polarization efficiencies on mobility. This efficiency is smaller for the gauche conformation. At 295 K all long side chains are in the gauche conformation.

A careful look at the aliphatic region of the spectra in Figure 10 shows that the peak at ~14 ppm, which belongs to the CH_3 end groups, suffers from a continuous decrease of the signal to noise ratio. The reason for this behavior is the increasing velocity of the methyl group rotation which causes a severe loss in cross-polarization efficiency.[8a] Within the region between 22 and 28 ppm one broad peak can be seen at low temperatures. At higher temperatures this broad peak

Table 2. Chemical Shifts of the ^{13}C Peaks of OM-30 at Various Temperatures (Adamantane Low-Field Peak at 38.5 ppm as Reference)

T (K)	CO amide	CO ester	OCH_2	C_α	OCH_3	int CH_2	int CH_2	δ-CH_2	C_{17}[a]	C_{18}
243	175.9	172.4	64.5	56.9	51.5	32.6	30.7	25.8	23.2	14.4
255	175.9	172.4	64.4	57.1	51.5	32.6	30.6	25.9	23.2	14.4
273	175.9	172.3	64.3	57.1	51.5	32.6	30.3	25.9	23.2	14.4
290	175.9	172.3	64.1	57.1	51.5	32.4	30.0	25.9	22.9	14.4
320	175.9	172.0	64.1	57.1	51.2		29.9	25.9	22.9	

[a] As shoulder of the δ-peak.

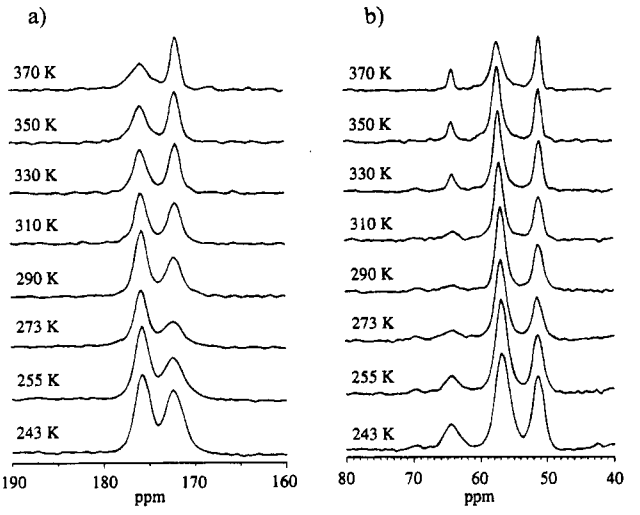

Figure 11. VT-^{13}C-CP/MAS-NMR of OM-30-2100 measured between 243 and 370 K: (a) ester (172 ppm) and amide groups (176 ppm): (b) OCH_3 (52 ppm), C_α (57 ppm), and OCH_2 (65 ppm) groups. These experiments allow determination of the temperature at which the relaxation frequency of the groups reaches 70 kHz.

is split into two distinct peaks of which the small one (~22.8 ppm) is assigned to the CH_2 group neighboring the methyl end group of the alkyl side chain (C_{17}). Again, the reason for this splitting and the narrowing of the broad peak is motional narrowing at higher temperatures. The peak assignment for the broad peak, ~26 ppm, is not as straightforward as it is for the peaks at higher field. At low temperatures at least two different CH_2 groups contribute to that peak: δ-CH_2 and C_{17} in a mostly all-trans environment.[8a] The latter contribution vanishes at higher temperatures because the "far" chain ends are the first sites within the molecule to be affected by growing disorder and thereby a loss of all-trans states. However, the interior δ-CH_2 is also moving faster, evident by the peak narrowing.

If one looks at the behavior of the ester carbonyl peak at ~172 ppm as a function of temperature from 243 to 370 K (Figure 11a), it can be seen that the line broadens up to 270 ± 10 K and then becomes narrower again. For the sake of clarity only steps of 20 K are shown; the experiment itself was done in steps of 10 K. The broadening arises as the motion of the ester group becomes comparable to the frequency of the proton decoupling field.[34,35] According to Rothwell and Waugh,[36] the profile of line width vs temperature shows a maximum where the correlation time for molecular motion, τ_c, is equal to the modulation period of the decoupling (ω_1^{-1}). In the "short-correlation" limit ($\omega_1\tau_c \ll 1$), i.e., at high temperatures, the line width is reduced by the rapid motional averaging, while in the "long-correlation" limit ($\omega_1\tau_c \gg 1$), i.e., at low temperatures, the line width is reduced by efficient decoupling of C−H dipolar interactions. In the experiment presented here, the frequency of the decoupling field was ~70 kHz. That means that the ester group undergoes a motion at a relaxation rate of about 70 kHz at 270 K.

A similar behavior can be observed for the OCH_2 peak (Figure 11b; ~65 ppm), where the minimum intensity and the maximum line width are reached at slightly higher temperatures of 280 ± 10 K. The same statement is valid for the OCH_3 group (Figure 11b, ~52 ppm). The relaxation rate for both OCH_2 and OCH_3 is therefore ca. 70 kHz at about 280 K. Because of the uncertainty in detecting the exact position of the minimum of intensity, this shift of 10 K between OCH_2 and the ester group does not allow any further conclusions.

Neither the amide (Figure 11a; ~176 ppm) nor the C_α (Figure 11b, ~57 ppm) resonance of the α-helical backbone shows a similar behavior. That means that the main chain does not undergo any local kilohertz motion at temperatures between 243 and 370 K. The chemical shifts of the CO amide and C_α peak are unchanged by temperature; therefore the molecule has an α-helical structure within the whole temperature region.

CP/MAS Experiment at Low Sample Spinning Frequency. It was realized some time ago that spinning a powder sample about an axis inclined at the magic angle with respect to the magnetic field will average the chemical shift anisotropy to zero, the general condition for complete averaging being that the spinning rate exceeds the breadth of the shift anisotropy. Thereby it is possible to obtain high-resolution ^{13}C spectra of solids. Nevertheless high resolution is achieved at the expense of the information contained in the chemical shift anisotropy. By reducing the spinning speed, a compromise can be reached. When the spinning speed is less than the chemical shift anisotropy, the isotropic line in the NMR spectrum is flanked on both sides by sidebands spaced at the spinning frequency.

In our case, the purpose of measuring CP/MAS spectra at a moderate spinning frequency (~1.1 kHz) was to find out whether one of the carboxyl peaks (main chain amide or side chain ester) changes the slope of its chemical shift tensor. The result is shown in Figure 12. If one looks carefully at the sideband envelope of both CO peaks, it can be seen easily that there is no change in the appearance of the sideband pattern of the amide peak. The only change of that pattern is a continuous loss of signal intensity due to less effective cross polarization at higher temperatures. On the other hand, a dramatic change of the sideband pattern of the ester peak can be observed. Whereas the most intense peak at 235 K is one of its sidebands, the isotropic line itself has the highest intensity at room temperature. That means that a severe change in the shape of the ester chemical shift tensor takes place as the temperature is increased from 235 to 292 K. The reason for the nearly unchanged amide tensor and the drastically changed ester tensor is a different motional behavior of the two different sites. Whereas the ester group

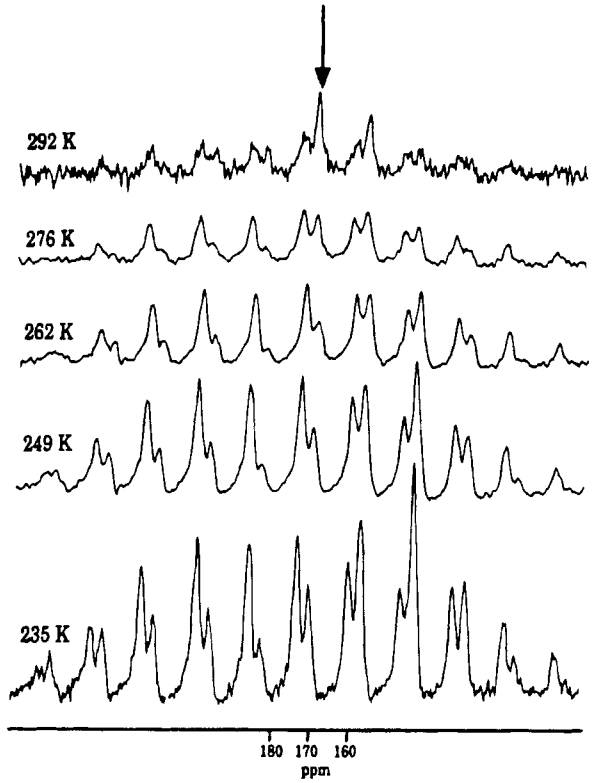

Figure 12. VT-^{13}C-CP/MAS-NMR of the ester and amide groups of OM-30-2100 measured between 235 and 292 K. The zero-order ester peak is marked by an arrow. The spinning frequency is 1.1 kHz in this experiment.

changes its local motion, the amide group seems to be unaffected by a rise in temperature.

4. Discussion

4.1. Ordered Side Chains. To explain the behavior of the integral intensity, Q, the structure was modeled by three separate constituents: the helices, the crystalline side chains, and the amorphous side chains. The normalized invariant Q can be written with this three-phase model as[32,37]

$$\left(\frac{Q(T)}{Q(293\ \mathrm{K})}\right)^{1/2} 1 + (T - 293\ \mathrm{K})(\sum_i \kappa_i \theta_i) \qquad (7)$$

where the constant κ_i's depend on the three volume fractions and densities at 293 K. The θ_i's are the volume expansion factors of the different volume parts. A change of the slope therefore indicates a change in the volume expansion factors. The noncontinuous change of the volume expansion factors can be explained as a transition at about 293 ± 5 K. A similar behavior of the integral invariant Q was found for PBLG and PMLG and explained as an onset of side chain motion.[6,37]

Reported melting points for OM-x, $x \geq 52\%$,[12b] allow extrapolation of a linear dependence of the melting point T_m from the long alkyl chain portion, x:

$$T_m(x) = 264\ \mathrm{K} + 0.85x\ \mathrm{K} \qquad (8)$$

For $x = 30$ the melting point can be approximated to 290 K. This value corresponds very well to the 293 ± 5 K value we find from the SAXS experiments. NMR shows that at 295 K all long alkyl chains are in a gauche conformation; the "all-trans" peak is no longer visible. The minimum of the DSC transition is at 273 K. The relaxation strengths of the α- and β-processes change at ca. 285 K. These results, together with the coexistence of an amorphous halo and a crystalline peak in the WAXS experiment, allow us to conclude that there are amorphous and crystalline side chain parts in OM-30 and that the melting of the crystals is completed at about 293 ± 5 K. It was determined from WAXS that only about 6 side chains form a crystallite at 260 K, and NMR confirms that the side chains in OM-30 are not as highly ordered as in POLG.

4.2. Identification of the β-Relaxation. Comparison with the literature allowed identification of the γ-process as a restricted twisting motion of the ester dipoles in the side chains. Two dynamical glass transitions, α and β, were observed in the present study. We will focus first on the β-relaxation.

The ^{13}C-CP/MAS-NMR experiment showed that the relaxation frequency of the ester group in the side chain is 70 kHz at 270 ± 10 K. This NMR result for the ester group is plotted in Figure 8 (open square). The graphic comparison in Figure 8 with the three processes measured by DS shows immediately that the ester group is responsible for the β-process. The α-relaxation is much slower at 273 K we find 50 Hz, a factor of 1000 slower compared to the β-relaxation. The ester groups therefore undergo a dynamical glass transition. The approximated calorimetric glass transition temperature of 238 K agrees quite well with the onset of the second transition in the DSC measurements (230−240 K). The kilohertz frequency region of the β-transition around room temperature is in agreement with the results for other polypeptides in the solid state from the literature, especially for PBLG.[6]

We have to note here that, in general, relaxation times determined with NMR and DS are not identical. Usually, the dielectric relaxation times are higher,[38] with $3\tau_{NMR} = \tau_{DS}$ for spherical molecules.[39] The agreement between NMR and DS is therefore very good in our case, which may caused by the specific functional groups investigated here.

To determine if both side chain dipoles in the short and long chains belong to this β-transition, the dynamics of the groups OCH_3 and OCH_2, adjacent to the ester groups in the different side chains, were investigated. The VT-NMR for these two groups, given in Figure 11b, shows that both OCH_3 and OCH_2 have a relaxation rate of 70 kHz at 280 ± 10 K. This NMR result is plotted in Figure 8 (open circle) to compare it with DS. Within the errors of the experiment, this is identical with the result for the ester group COO (270 K). The side chain region next to the ester dipole has the same frequency of 70 kHz for both the long and short chains at about 280 K. The β-relaxation is therefore caused by the ester dipoles in the long and short side chain. This is in agreement with the literature, where for other copolyglutamates only one β-relaxation was found for the different side chain dipoles.[2a,6] This single process was assigned to a cooperative, large-scale motion of the whole side chain.[6,7b,8c,d,10a−c] The contribution of both side chains to the β-relaxation also explains why the relaxation strength of this transition increases until the melting point of the side chains is reached. Only comletely amorphous side chains can contribute to the β-relaxation. With increasing temperature more long side chains melt and can therefore contribute to the relaxation and increase the relaxation strength. Beyond the melting point the relaxation strength follows eq 2 with a constant dipole density, i.e., is constant within

the limited temperature window for our experiment.

It is known that copolymerization of hexyl glutamate and methyl glutamate[2a] as well as methyl glutamate and benzyl glutamate[6] increases the transition temperature of the β-processes compared to the homopolymers. The glass temperature for OM-30 is within the experimental error identical to that of PMLG.[8d] The NMR results show that the β-process belongs to both side chains, but its glass temperature is controlled by the short side chains.

At 293 K the dielectric relaxation frequency of the side chain dipole is about 2 MHz, while the relaxation frequency of alkanes (dodecane) in the melt is ca. 19 GHz (at about 300 K).[40] The reduced degrees of freedom of the anchored side chain strongly reduce the relaxation frequency. Our current NMR results show that the far end of the side chain is much faster. Yamaguchi et al. found for different copolyglutamates that the far end of the long side chain reaches the mobility of alkane melts.[13]

Having identified the side chain dipoles as the cause of the β-relaxation, it is possible to approximate the dipole moment, μ, of the side chains from $\Delta\epsilon_\beta$ and the structural data. Equation 2 allows calculation of an effective dipole moment, $\mu_{eff} = (\delta\langle\mu\rangle^2)^{0.5}$, with the result $\mu_{eff} = 1.6 \pm 0.6$ D at 293 K. This dipole moment is smaller than for a free ester group (1.8 D), but this is to be expected for side chain dipoles in peptides.[24] For PBLG a side chain dipole of 1.4 D was found.[10]

4.3. Origin of the α-Relaxation. Both side chain dipoles are involved in the β-process, but only the completely amorphous octadecyl side chains can contribute to this relaxation.[8d] It is therefore the question if the α-relaxation belongs to the side chain dipoles within crystalline octadecyl chains or if it is caused by the main chain dipoles.

For polyglutamate homopolymers of types I and II additional relaxations were found as shoulders in the γ- and β-relaxations.[8d] Only one of these transitions can be related to the α-relaxation in OM-30. In type I homopolymers a shoulder was present on the high-temperature side of the β-relaxation (see Figure 12 in ref 8d) and was assigned to the dipoles in the long side chains which are in the crystalline state before the melting temperature.[8d] Our NMR results show that both side chains contribute to the β-process. The α-process should therefore vanish after the melting of all side chains if the assignment to crystalline side chains is correct. We found that beyond the melting process the relaxation strength of the α-process is not equal to zero and the ratio to the β-relaxation is constant (see Figure 7). The α-process therefore cannot be assigned to the crystalline side chains. It could also be possible that the dipoles in long amorphous side chains surrounded by crystalline side chains are responsible for the α-process. The relaxation strength of such a process would be strongly reduced compared to the β-relaxation and would vanish if all the side chains are molten. Instead it is found that $\Delta\epsilon_\alpha$ is constant after the melting at 293. The side chains are therefore not responsible for the α-process in our dielectric spectroscopy experiments.

For POLG, with only long octadecyl chains, the relaxation frequency of the carbon atom C_α in the α-helix was determined by NMR and found to be 60 kHz at about 313 K.[8a,b] From DS experiments for OM-30 a frequency of 10 kHz at 313 K for the α-relaxation was found. This also fits the NMR results for C_α; the C_α relaxation has a frequency smaller than 70 kHz in the whole temperature range of our NMR experiment (up to 370 K). The order of magnitude for the α-process of OM-30 is therefore reasonable compared to the main chain motion in the related polymer POLG. The main chain motion in POLG is continuously increasing with temperature and does not show a discontinuity at the melting point of the side chains. The same is found for the α-process in OM-30 in the present study.

Several relaxations can be discussed for the rod. The main chain can show an accordion-like vibration, which changes the pitch of the α-helix locally. It is known from the NMR measurements that the helix is locally stiff; this vibration is therefore not the cause of the α-relaxation. The main chain as a whole can undergo an end-to-end rotation. This is very unlikely, because in the solid state each rod can be imagined as being caged between adjacent rods. There is no free volume available for an end-to-end rotation. Even for liquid-crystalline solutions the frequency for this relaxation is about 10 mHz at room temperature.[7b] But each rod can undergo a so-called "chop-stick" motion within the cage formed by its neighbors.[41] This type of motion was found in dielectric spectroscopy for different rodlike molecules.[41,42] Another possibility would be a restricted rotation of the whole rod around its long axis (libration) or a screw motion. These types of relaxations were found in PMLG.[9]

It will be shown in Appendix A that the assumption of a chop stick motion of the main chain can explain the ratio between the relaxation strength of the α- and β-processes. The understanding of this ratio is critical, because the dipole moment of the whole rod molecule (parallel to its long axis) is huge compared to single side chain dipoles, which are responsible for the β-relaxation. Experimentally both relaxation strengths are of the same order of magnitude. The assumption of a chop-stick motion of the whole main chain even makes it possible to calculate the order of magnitude for the time scale of the α-relaxation (see Appendix B). The calculations show the main chain to be slower by a factor of 1000 compared to the side chain motion, which is in agreement with the experimental results. In the case of a libration the dipole moment perpendicular to the main chain axis, which is unknown for OM-30, is important. In PBLG and PMLG no dipole moment perpendicular to the main chain axis was found; therefore it can be expected to be also extremely small for OM-30. This would explain the small value for $\Delta\epsilon_\alpha$. Calculations similar to those for the chopstick motion in the apprendix are not reliable for the libration, because of the small, unknown value of the dipole moment perpendicular to the long rod axis.

A hint as to which type of motion is responsible for the α-relaxation comes from the molecular weight (M_r) dependence of the DS results. The chopstick motion will roughly depend on the third power of the M_r, while the libration is linear in M_r.[43] The two polymers investigated with DS differ in average M_r by a factor of 2.2. The chopstick motion should hence be faster by a factor of 10, while the libration is expected to be just twice as fast for the small polymer. Experimentally both polymers show no significant difference in relaxation frequencies. This experimental result favors therefore the libration of the whole rod over a possible chopstick motion as a cause for the α-relaxation. To distinguish between the two possibilities of a libration or a chopstick

motion, we refer to an upcoming investigation with different solid-state NMR techniques.[44]

5. Conclusion

The side chains in OM-0 (PMLG, type II) are amorphous and show a β-transition at 273 K, while the main chain undergoes an α-process at 458 K. In OM-100 (POLG, type I), with only long octadecyl chains, the side chains are crystalline below the melting point of around 313 K. OM-30 shows a combination of the molecular dynamics in homopolymers of types I and II. Copolymerization of polyglutamate with methyl and octadecyl side chains leads to the coexistence of amorphous and crystalline side chains below the melting point of ca. 293 K. Both side chains contribute to a large-scale motion of the ester dipoles (β-relaxation), with a WLF-type temperature dependence. The main chain in OM-30 also undergoes a dynamic glass transition (α-relaxation). The glass temperatures approximated for both processes are within experimental accuracy identical and identical to the calorimetric glass temperature T_g of 238 K. The main chain mobility, i.e., the α-relaxation frequency, monotonously increases with temperature above the glass transition and shows no transition related to the melting of the crystalline side chains.

Yamaguchi et al.[13] proposed a layer model for the side chains in OM-x. The region close to the helix formed by the methyl groups and the inner parts of the octadecyl chains, and an outer part formed by the octadecyl chains. The outer part consists of amorphous and crystalline parts, even below $x = 35$. The mobility in the outer part of the side chains was measured quantitatively and was found to have gigahertz relaxation frequencies above the melting point, which is the same order of magnitude as for liquid alkanes.[13] Our work presented here allowed the quantification of the mobility of the side chain part close to the helix (side chain dipoles) and the helix itself. At room temperature (293 K) the relaxation frequency of the inner part of the side chains (ester dipoles) is in the megahertz region, while the main chain helix undergoes a process in the kilohertz region at room temperature. We found qualitatively that the mobility of the outer part of the long side chains is faster than the mobility of the side chain dipoles. The copolyglutamate OM-30 shows a hierarchy of mobilities, from the restricted motion of the rodlike helix and the glass transition of the side chain dipoles close to the helix to the melting of the crystalline octadcyl side chains and the subsequent liquidlike mobility of these long side chains.

Future work will concentrate on the measurement of the molecular dynamics in Langmuir–Blodgett films of OM-30. The comparison with the present investigation will allow determination of the influence of the structure and thickness of films of OM-30 on the molecular relaxations.

Acknowledgment. We thank B. Ewen, D. Johannsmann, H. W. Spiess, and M. Stamm for helpful discussion. Technical support from G. Zak and M. Bach is thankfully acknowledged.

Appendix A. Expected Ratio for the Relaxation Strength between the α- and β-Relaxation

The chopstick motion of the rods occurs in the "cage" spanned by their neighbor rods. The restriction of the rods into a small cage increases the frequency of the relaxation compared to an end-over-end rotation, but it also decreases the relaxation strength, because the whole dipole moment cannot contribute to the relaxation. It was found theoretically and experimentally that the relaxation strength depends on the angle χ by which the rod can rotate within its cage.[42]

$$\Delta\epsilon_\alpha - \Delta\epsilon_{rod}(1 - 0.25(1 + \cos\chi)^2) \qquad \text{(A1)}$$

$\Delta\epsilon_{rod}$ is the relaxation strength of the whole rod if it could move freely. The angle χ is given by the ratio of the rod length and the "cage" diameter. Both parameters are known from the structural data. The angle χ is equal to 0.5–0.6°, which means that $\Delta\epsilon_\alpha/\Delta\epsilon_{rod}$ is ca. 5×10^{-5}. The value $\Delta\epsilon_{rod}$ is unknown but can be related to $\Delta\epsilon_\beta$ with the help of eq 2:

$$\Delta\epsilon_{rod} \approx \Delta\epsilon_\beta \frac{\langle\mu_{rod}^2\rangle}{\langle\mu_{\beta,eff}^2\rangle} \qquad \text{(A2)}$$

It is known for PMLG and PBLG that the dipole moment per residue of the rod is about twice the dipole moment of the side chains.[23,24] Using this assumption (and the determined $\mu_{\beta,eff} = 1.6 \pm 0.6$ D), it follows from eq 12 that $\Delta\epsilon_\alpha$ is ca. 40 ± 15% of the side chain relaxation strength $\Delta\epsilon_\beta$. In the experiment a ratio of about 0.32 ± 0.08 above 285 K is found (see Figure 7). The assumption of a chopstick motion for the main chains leads to the same order of magnitude for the relaxation strength of the β-relaxation compared to the α-relaxation.

Appendix B. Expected Dynamics for the Chopstick Motion of the Main Chain

The relaxation time for the chopstick motion is given by[45]

$$\tau = \chi^2/D_{r0} \qquad \text{(B1)}$$

The angle χ is given in Appendix A. D_{r0} is the rotation diffusion constant of the rod in an isotropic environment, given by[45]

$$D_{r0} = \frac{3k_B T[\ln(L/d) - \varphi]}{\pi\eta_S L^3} \qquad \text{(B2)}$$

Here d is the diameter of the rod and η_S is the viscosity of the environment in which the rod moves, which is the side chain matrix in the present case. The parameter φ is of order 1 and will be neglected in the following. All the parameters necessary to calculate the relaxation time τ of the main chain are known, except for the viscosity. To approximate this value, the alkyl side chain relaxation time τ_β from the β-relaxation of the DS experiments can be related to the viscosity:[43]

$$\tau_\beta = \frac{\eta_S R_g^3}{k_B T} \qquad \text{(B3)}$$

The radius of gyration, R_g, of the side chains can be approximated assuming an all-trans configuration.[45]

$$R_g^2 = l^2/12 \qquad \text{(B4)}$$

where l is length of the octadecyl side chain in the all-trans conformation. With these equations, the main chain relaxation time can be written as a function of the side chain relaxation time:

$$\tau = \tau_\beta \frac{L^3 \pi \chi^2}{3 \ln(L/d) R_g^3} \quad \text{(B5)}$$

With these approximations and assumptions, the main chain relaxation time is calculated to be slower by a factor of 1000, which agrees with the experimental data.

References and Notes

(1) Wegner, G. *Mol. Cryst. Liq. Cryst.* **1993**, *235*, 1.
(2) (a) Watanabe, J.; Fukuda, Y.; Gehani, R.; Uematsu, I. *Macromolecules* **1984**, *17*, 1004. (b) Watanabe, J.; Ono, H.; Uematsu, I.; Abe, A. *Macromolecules* **1985**, *18*, 2141. (c) Watanabe, J.; Takashina, Y. *Macromolecules* **1991**, *24*, 3423. (d) Watanabe, J.; Takashima, Y. *Polym. J.* **1992**, *24*, 709. (e) Watanabe, J.; Goto, M.; Nagase, T. *Macromolecules* **1987**, *20*, 298.
(3) Duda, G.; Schouten, A. J.; Arndt, T.; Lieser, G.; Schmidt, G. F Bubeck, C.; Wegner, G. *Thin Solid Films* **1988**, *159*, 221.
(4) Schmidt, A.; Mathauer, K.; Reiter, G.; Foster, M. D.; Stamm, M.; Wegner, G.; Knoll, W. *Langmuir* **1994**, *10*, 3820.
(5) Elliott, A.; Fraser, R. D.; MacRae T. P. *J. Mol. Biol.* **1965**, *11*, 821.
(6) Tsutsumi, A.; Hikichi, K.; Takahashi, T.; Yamashita, Y.; Matsushima, N.; Kanke, M.; Kaneko, M. *J. Macromol. Sci. Phys.* **1973**, *B8* (3–4), 413.
(7) (a) Murthy, N. S.; Samulski, E. T.; Know, J. R. *Macromolecules* **1986**, *19*, 941. (b) Adachi, K.; Hirose, Y.; Ishida, Y. *J. Polym. Sci., Polym. Phys. Ed.* **1975**, *13*, 737.
(8) (a) Yamanobe, T.; Tsukahare, M.; Komoto, T.; Watanabe, J.; Ando, I.; Uematsu, I.; Deguchi, K.; Fujito, T.; Imanari, M. *Macromolecules* **1988**, *21*, 48. (b) Mohanty, B.; Watanabe, J.; Ando, I.; Sato, K. *Macromolecules* **1990**, *23*, 4908. (c) Romero Colomer, F. J.; Gomez Ribelles, J. L.; Lloveras, Macia, J.; Munoz Guerra, S. *Polymer* **1991**, *32*, 1642. (d) Romero Colomer, F. J.; Gomez Ribelles, J. L.; Barrales-Rienda, J. M. *Macromolecules* **1994**, *27*, 5004.
(9) Sasaki, S.; Takiguchi, Y.; Kamata, M.; Uematsu, I. *Polymer* **1979**, *20*, 71.
(10) (a) Nakamura, H.; Mashimo, S.; Wada, A. *Macromolecules* **1981**, *14*, 1698. (b) Mori, Y.; Ookubo, N.; Hayakawa, R.; Wada, Y. *J. Polym. Sci., Polym. Phys. Ed.* **1982**, *20*, 2111. (c) Romero Colomer, F.; Gomez Rebelles, L. *Polymer* **1989**, *30*, 849. (d) Yamaguchi, M.; Tsutsumi, A. *Polym. J.* **1993**, *25*, 131.
(11) Shoji, A.; Ozaki, T.; Saito, H.; Tabeta, R.; Ando, I. *Macromolecules* **1984**, *17*, 1472.
(12) (a) Tsujita, Y.; Ojika, R.; Tsuzuki, K.; Takizawa, A.; Kinoshita, T. *J. Polym. Sci., Part A: Polym. Chem.* **1987**, *25*, 1041. (b) Tsujita, Y.; Ojika, R.; Takizawa, A.; Kinoshita, T. *J. Polym. Sci., Part A: Polym. Chem.* **1987**, *25*, 1041.
(13) Yamaguchi, M.; Tsutsumi, A. *Polym. J.* **1990**, *22*, 781.
(14) Mathy, A.; Mathauer, K.; Wegner, G.; Bubeck, C. *Thin Solid Films* **1992**, *215*, 98.
(15) Elliot, A.; Malcom, B. R. *Proc. R. Soc. London* **1959**, *A249*, 30.
(16) Mathauer, K. Ph.D. Thesis, Mainz, 1991.
(17) Schmidt, A. Ph.D. Thesis, Mainz, 1993.
(18) Porod, G. *Monstsh. Chem.* **1949**, *80*, 251.
(19) Kratky, O. *Z. Elektrochem.* **1954**, *58*, 49.
(20) Strobl, G. R. *Acta Crystallogr.* **1970**, *A26*, 367.
(21) Pugh, J.; Ryan, T. J. *IEEE Conf. Dielec. Mater., Meas. Appl.* **1979**, *144*, 404.
(22) Kremer, F.; Boese, D.; Meier, G.; Fischer, E. W. *Prog. Colloid Polym. Sci.* **1989**, *80*, 129.
(23) Takashima, S. *Electrical Properties of Biopolymers and Membranes*; Adam Hilger: Bristol, 1989.
(24) Wada, A. *Adv. Biophys.* **1976**, *9*, 1.
(25) (a) Havriliak, S.; Negami, S. *J. Polym. Sci., Part C* **1966**, *14*, 99. (b) Havriliak, S.; Negami, S. *Polymer* **1967**, *8*, 161.
(26) (a) Riande, E.; Saiz, E. *Dipole Moments and Birefringence of Polymers*; Prentice-Hall: Englewood Cliffs, NJ, 1992. (b) Boettcher, C. J. F.; Bordewijk, P. *Theory of Electric Polarization*; Elsevier: Amsterdam, 1978; Vol. 2.
(27) Onsager, L. *J. Am. Chem. Soc.* **1936**, *58*, 1486.
(28) Mott, N. F.; Davis, E. A. *Electronic Processes in Noncrystalline Materials*; Clarendon Press: Oxford, 1979.
(29) Williams, M. L.; Landel, R. F.; Ferry, J. D. *J. Am. Chem. Soc.* **1955**, *77*, 3701.
(30) (a) Mueller, D.; Kricheldorf, H. R. *Polym. Bull.* **1981**, *6*, 101. (b) Kircheldorf, H. R.; Mueller, D. *Macromolecules* **1983**, *16*, 615. (c) Saito, H.; Tabeta, R.; Shoij, A.; Ozaki, T.; Ando, I. *Macromolecules* **1983**, *16*, 1050.
(31) (a) Meirovitch, E.; Samulski, E. T.; Leed, A.; Scheraga, H. A.; Rananavare, S.; Nemethy, G.; Freed, J. H. *J. Phys. Chem.* **1987**, *91*, 4840. (b) Yamazaki, T.; Abe, A. *Polym. J.* **1987**, *19*, 777. (c) Abe, A.; Yamazaki, T. *Macromolecules* **1989**, *22*, 2138.
(32) Feigin, L. A.; Svergun, D. I. *Structure Analysis by Small-Angle X-ray and Neutron Diffraction*; Plenum Press: New York, 1987.
(33) VanderHart, D. L. *J. Magn. Reson.* **1981**, *44*, 117.
(34) Lyerla, J. R.; Yannoni, C. S.; Fyfe, C. A. *Acc. Chem. Res.* **1982**, *15*, 208.
(35) Yannoni, C. S. *Acc. Chem. Res.* **1982**, *15*, 201.
(36) Rothwell, W. P.; Waugh, J. S. *J. Chem. Phys.* **1981**, *74*, 2721.
(37) Matushima, N.; Hikichi, K. *Polym. J.* **1978**, *10*, 437.
(38) Bloembergen, N.; Purcell, E. M.; Pound, R. V. *Phys. Rev.* **1948**, *73*, 679.
(39) Connor, T. M. *Trans. Faraday Soc.* **1964**, *60*, 1574.
(40) (a) Granick, S. *Science* **1991**, *253*, 1374. (b) Hu, H.-W.; Carson, C. A.; Granick, S. *Phys. Rev. Lett.* **1991**, *66*, 2758.
(41) Mori, Y.; Ookubo, N.; Hayakawa, R.; Wada, S. *J. Polym. Sci., Polym. Phys. Ed.* **1982**, *20*, 2111.
(42) (a) Moscicki, J. K.; Williams, G.; Aharoni, S. M. *Macromolecules* **1982**, *15*, 642. (b) Moscicki, J. K.; Williams, G. *J. Polym. Sci., Polym. Phys. Ed.* **1983**, *21*, 197. (c) Moscicki, J. K.; Williams, G. *J. Polym. Sci., Polym. Phys. Ed.* **1983**, *21*, 213.
(43) Bur, A. J.; Roberts, D. E. *J. Chem. Phys.* **1969**, *51*, 406.
(44) Lehmann, S.; Schmidt, A.; Boeffel, Ch.; Spiess, H. W., in preparation.
(45) Doi, M.; Edwards, S. F. *The Theory of Polymer Dynamics*; Clarendon Press: Oxford, 1989.

MA9500289